Electronic Supplementary Material (ESI) for Polymer Chemistry.

SUPPORTING INFORMATION

Tacticity dependent cross-plane thermal conductivity in molecularly engineered amorphous polymers

Jaekyo Lee,‡[a] Youngmu Kim,‡[b,c] Shalik Ram Joshi,[a] Min Sang Kwon[b,c,*] and Gun-Ho Kim [a,*]

[a] *Department of Mechanical Engineering, Ulsan National Institute of Science and Technology (UNIST), Ulsan 44919, South Korea.*

[b] *Department of Materials Science and Engineering, Ulsan National Institute of Science and Technology (UNIST), Ulsan 44919, South Korea.*

[c] *Department of Materials Science and Engineering, Seoul National University, Seoul 08826, South Korea.*

‡ *These authors contributed equally to work.*

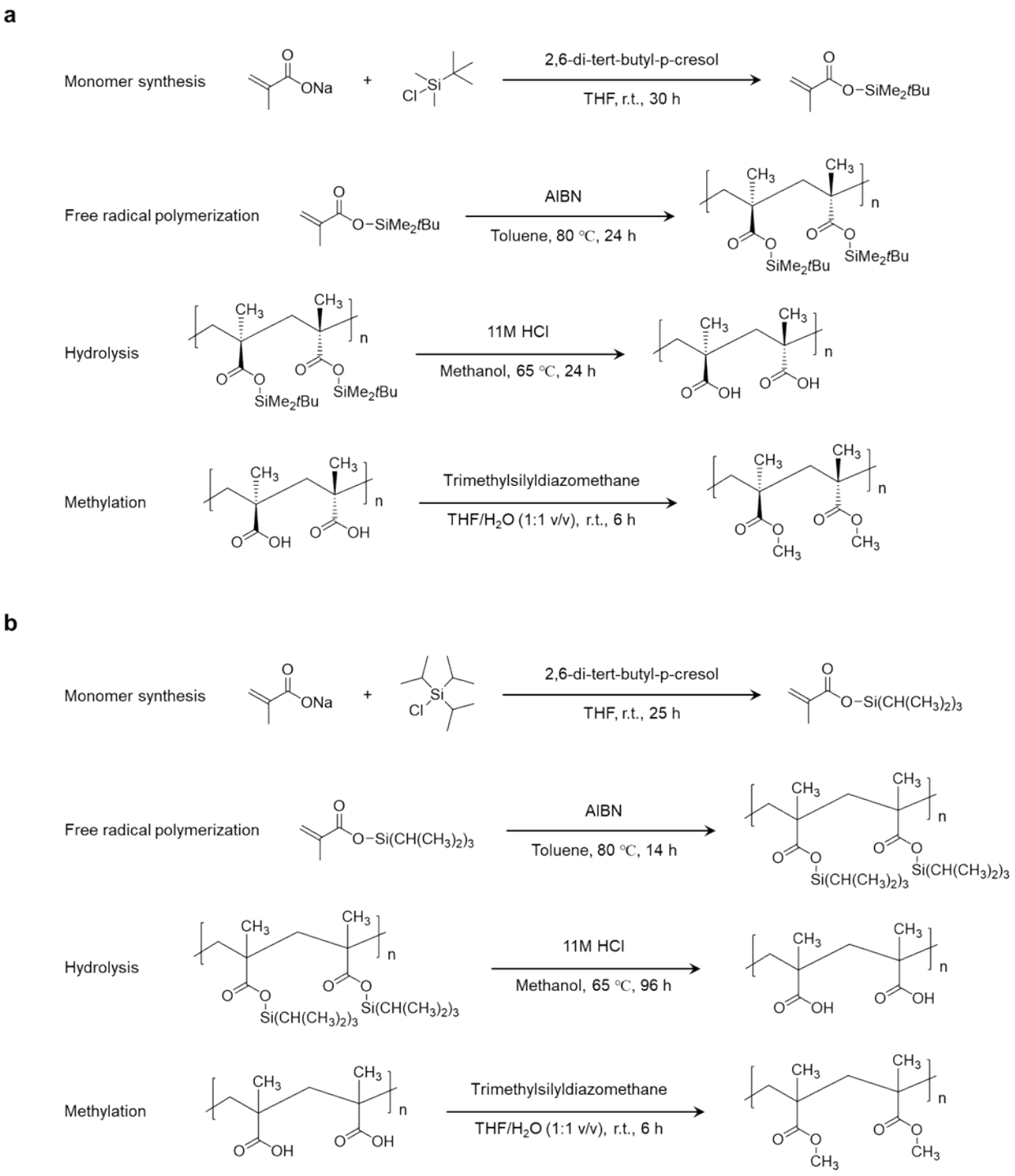

Fig. S1. Synthesis of polymers | Reaction scheme for (a) synthesis of *s*-PMAA and (b) synthesis of *a*-PMAA.

Molecular Weight Measurement

The molecular weights and dispersity of PMMAs (obtained from PMAAs) were measured by GPC. The GPC (Young Lin YL9100 HPLC system) coupled with a refractive index (RI) detector (Young Lin YL9170 RI detector) and three columns were used. Tetrahydrofuran (THF, Samchun Chemicals, HPLC grade, stabilized, >99.9%) was used as the eluent at 35 ℃ with a flow rate of 0.8 mL/min. PMMA standards were used for calibration of RI signal.

Polymer	Major tacticity	Triad ratio[b] (rr/mr/mm)	M_n (D_a)	M_w (D_a)	PDI	Vendor
PMAA	Syndiotactic	**62**/27/11	19,800[b]	34,400[b]	1.74[b]	Our Lab Synthesized
	Atactic	34/**43**/23	22,300[b]	35,600[b]	1.59[b]	Our Lab Synthesized
	Isotactic	4/22/**74**	29,200[b]	36,700[b]	1.25[b]	Polymer Source
PAA	Atactic	26/**49**/25	57,500[1]	100,000[c]	1.74[1]	Sigma Aldrich
	Isotactic	7/30/**63**	49,000[c]	63,700	1.3[c]	Polymer Source

a. See Experimental Section for complete synthesis procedure. b. Measured after methylation. c. Values from the vendor. 1. Reference provided at the end of the ESI†

Table S1. Polymers used in this work | Overall information about polymers used in this work.

Differential 3ω Method

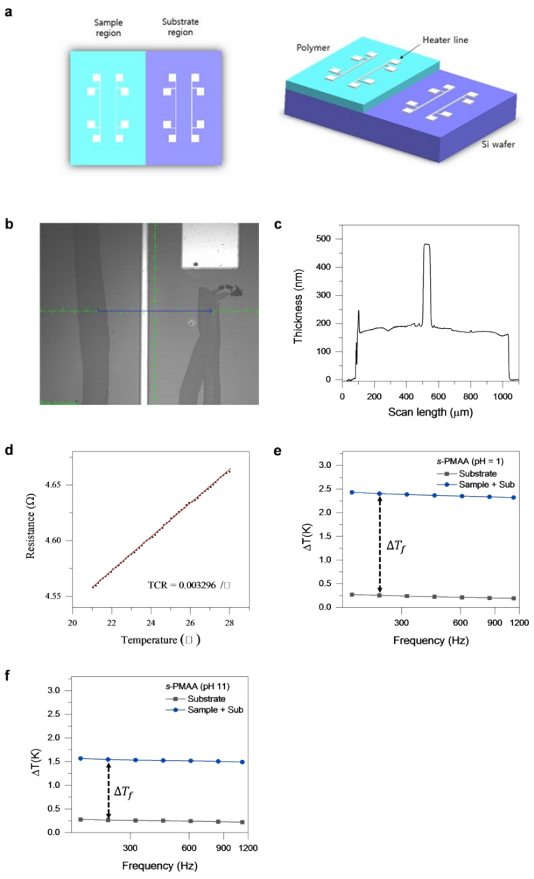

Fig. S2. Differential 3-omega measurement of thermal conductivity | (a) Sample configuration for the 3-omega measurement. Heater lines are deposited after half part of the sample is removed. (b) Optical view of sample surface while thickness measurement. (c) Sample thickness of nearby the heater line was measured by the surface profiler. (d) TCR value was calculated by measuring resistance while increasing the temperature of the heater line. (e-f) Temperature rise on sample and reference regions.

A differential 3-omega method is used for measuring the cross-plane thermal conductivity of polymer thin films. It has shown to be a reliable thermal conductivity measurement technique for similar film thicknesses and thermal conductivity.[2] It should be noted that the cross-plane thermal conductivity in spun cast polymer films is typically smaller than the in-plane one, and the observed enhancement represents conservative estimation. By applying the first harmonic AC current to the heater line, it generates heat through the heater line and creates a temperature difference between the heater and the underneath substrate. Temperature rise through the cross-planes direction is proportional to the change of third harmonic voltage on the heater.

$$\Delta T = \frac{2V_{3\omega}}{V_{1\omega}\beta_h}$$

Where, β_h is the temperature coefficient of resistance (TCR) for the heater line, $V_{1\omega}$ is applied first harmonic voltage and $V_{3\omega}$ is a measured third harmonic voltage.

The temperature rises in the sample (ΔT_s) and reference region (ΔT_r)are extracted by measuring the first and third harmonic voltage between inner pads (interesting part) with a lock-in amplifier (SR830 Lock-in Amplifier, Stanford Research Systems). By subtraction between temperature rise in sample and reference region, we calculate the temperature rise across the thin film (ΔT_f).

$$\kappa = \frac{P_h L}{A\Delta T_f} = \frac{P_h t_f}{w_h l_h \Delta T_f}$$

Where P_h represents Joule heating power generated by the heater line, t_f represents the thickness of polymer film thickness and w_h, l_h are the width and length of the heater line.

1-D heat transfer model based on Fourier's law is used to calculate cross-plane thermal conductivity. This model is satisfied because the width of the heater line (50 μm) is much larger than the thickness of polymer film (0.15 μm ~ 1.8 μm). The heater line is deposited 5 nm adhesion layer (Cr) and 300 nm of heater line material (Ag) by using an e-beam evaporator on the polymer film. The geometry of the heater line is precisely controlled by using a shadow mask for deposition.

For the deposited polymer film, the thermal excitation frequency range was selected to satisfy the line source approximation adapted in the thermal model. To satisfy the 1D heat diffusion model, the thermal penetration depth should be much greater than the heater line half width ($b = w/2 = 25.25\ \mu m$) which can be calculated by the following equation:

$$r = \sqrt{\frac{D}{4\pi f}}$$

Where r represents the thermal penetration depth and D represents thermal diffusivity of the silicon substrate (Silicon: 80 mm^2/s, silicon dioxide: 0.83 mm^2/s).

Using this equation, the lower and upper bound of thermal penetration depth was observed to be 75.36 μm for 1121 Hz and 195.25 μm for 167 Hz for the silicon and 7.68 μm for 1121 Hz and 19.89 μm for 167 Hz for silicon dioxide. Meanwhile, the upper bound of thermal penetration depth is well below the substrate thickness (675 μm), validating the 1 dimensionality of the heat diffusion model.

The Thickness of the film was measured by using surface profiler (KLA Tencor, P6). To minimize the error, a reference point was created by scratching the polymer film near to the heater line by a steel blade, of which the thickness is known by the used deposition parameter. The film thickness was measured at four different locations

(near to each heater line) to check the uniformity of the polymer film, and their standard deviation (σ_t) was found to be 1.32%, which supports the film uniformity. The thickness of each heater line was also measured simultaneously and found to be consistent with the deposition parameter (300 nm). The roughness values (R_a) of the polymer surface was calculated using the line profile (Fig. S2b) and were found to be much less than the film thickness (i.e., average 1.35% of the film thickness as seen in Table S2).

Polymer	Tacticity	pH	R_a (nm)	R_a / Thickness (%)
PMAA	Syndiotactic	1	11.85±0.78	0.87±0.05
		4	17.78±1.77	1.47±0.26
		7	1.2±0.54	1.18±0.46
		9	1.89±0.96	1.75±0.97
		11	18.27±13.41	1.26±0.97
	Atactic	1	1.31±0.45	2.37±0.93
		4	0.91±0.02	1.78±0.29
		7	3.33±0.41	2.04±0.09
		9	1.25±0.23	2.36±0.39
		11	1.66±0.34	3.05±0.09
	Isotactic	8	5.97±1.24	0.49±0.11
		9	23.16±5.44	1.61±0.40
		10	24.47±6.26	1.1±0.32
		11	16.46±7.53	1.26±0.60
PAA	Atactic	1	11.01±5.53	0.45±0.23
		4	20.83±7.20	0.72±0.25
		7	22.61±9.25	0.87±0.36
		9	19.13±4.19	1.08±0.21
		11	13.77±6.82	0.34±0.17
	Isotactic	1	13.71±2.45	0.81±0.15
		4	37.06±18.49	1.89±0.98
		7	12.97±7.09	0.87±0.22
		9	15.55±7.27	0.86±0.34
		11	22.56±9.76	1.57±0.45

Table S2. Data table containing roughness (R_a) value for each tacticity and pH.

The uncertainty of the measured thermal conductivities was calculated by the uncertainties of the film thickness, the heater line width, and the heater line TCR. The uncertainty of the heater line width ($\sigma_{SD,w}$) was weighted by a factor of $(\Delta T_s{}^2 + \Delta T_r{}^2)^{1/2}/\Delta T_f$ to reflect the fact that $\sigma_{SD,w}$ affects ΔT_s and ΔT_r independently. The temperature coefficient of resistance was calculated by measuring the resistance while gradually increasing the temperature of the heater line using a temperature controller.

Calculation for the degree of Ionization using FT-IR Spectroscopy

FT-IR spectra were measured on a Varian 670 spectrometer using a specular reflectance accessory at a grazing angle of 45°. 512 scans were recorded for each sample to obtain good signal to noise ratio. 5 different samples were utilized to check the reproducibility of the data. Peak analysis is operated by Gaussian function with 3 or 4 peaks were used to fit the PMAA and PAA spectra. While the baseline was user defined, the peak position and area under the curve (A_{peak}) was calculated by the software. Fig. S3 shows the FT IR data obtained from the instrument. The representative spectra which includes all the deconvoluted peaks is shown in Fig. S4. The asymmetric carboxylate (−COO^-) stretching band (1500 to 1620 cm^{-1}, peak 1 and 2 of deconvoluted peaks; see Fig. S4) and the carbonyl (−C=O) stretching band (1640 to 1760 cm^{-1}, peak 3 and 4 of deconvoluted peaks; see Fig. S4) of the carboxyl groups (−COOH) were used for peak analysis. Films at pH 1 and 4, carboxyl group bands are dominant which refers to less degree of ionization. As the degree of ionization increased further, carboxylate bands became dominant. The degree of ionization was calculated by the proportion of peak area.

$$\alpha = \frac{A_{COO^-}}{A_{COO^-} + A_{COOH}} \times 100\% = \frac{(A_{peak\,1} + A_{peak\,2})}{(A_{peak\,1} + A_{peak\,2}) + (A_{peak\,3} + A_{peak\,4})} \times 100\%$$

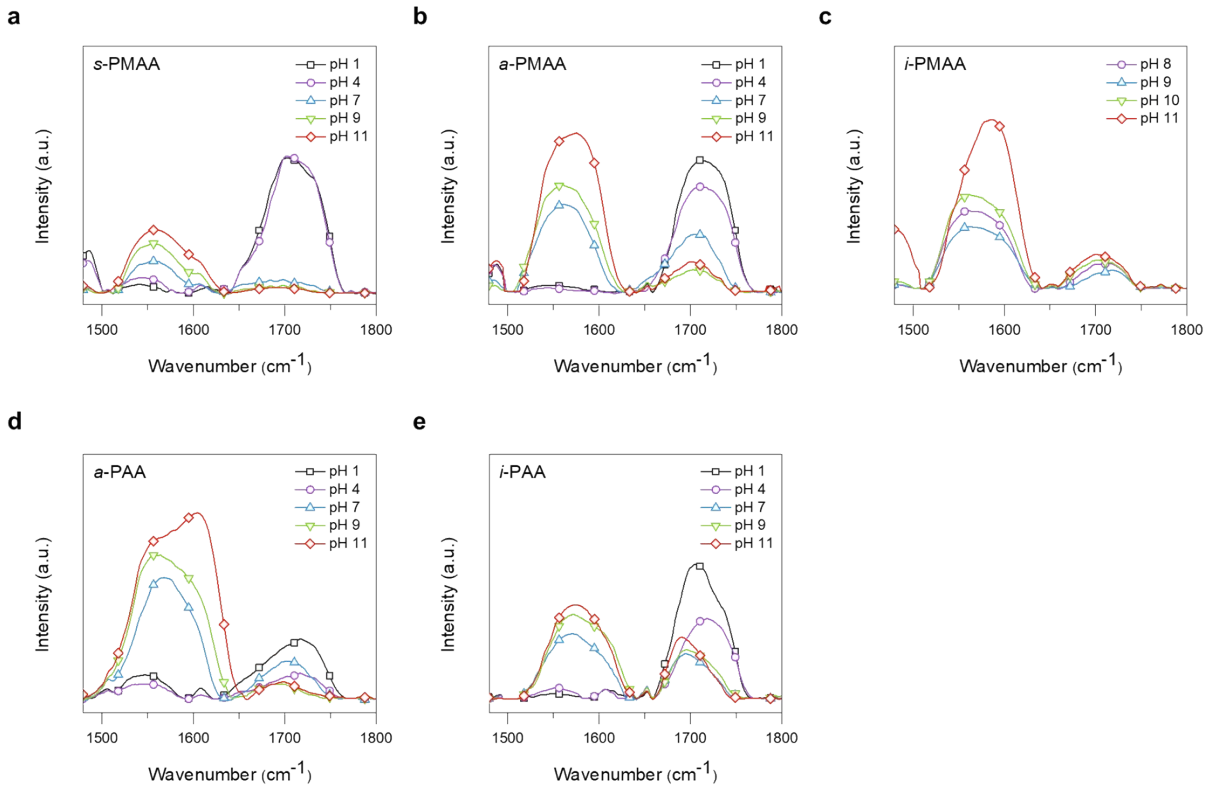

Fig. S3. FT-IR spectroscopy analysis | (a-c) FT-IR spectrum of PMAA and (d-e) PAA samples. Peaks were fitted assuming Gaussian distribution. The decrease in intensity of the carboxyl group (–COOH) stretching bands (1640 to 1760 cm^{-1}) with pH and the increase in the intensity of the asymmetric carboxylate ($–COO^-$) stretching bands (1500 to 1620 cm^{-1}) indicate ionization of the PMAA and PAA chains.

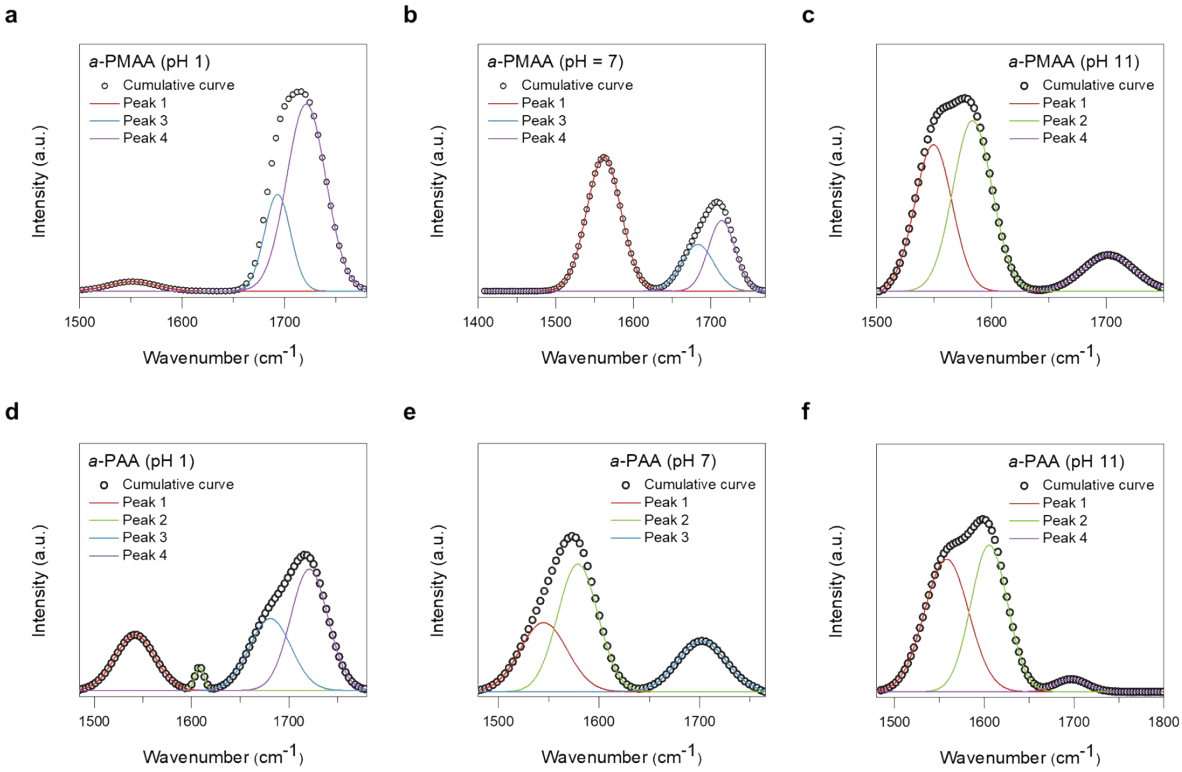

Fig. S4. Representative FT-IR spectra for PMAA and PAA with deconvoluted peaks | (a-c) FT-IR spectrum of *a*-PMAA samples. (d-f) FT-IR spectrum of *a*-PAA samples. Peak 1 (1500 to 1600 cm^{-1}) refers the low-frequency carboxylate ($-COO^-$) bands, peak 2 (1520 to 1620 cm^{-1}) refers to asymmetric carboxylate stretching bands, peak 3 (1640 to 1750 cm^{-1}) refers to self-associated hydrogen bonding carbonyl stretching bands of carboxyl groups (−COOH) and peak 4 (1660 to 1760 cm^{-1}) to non H-bonded carbonyl stretching bands of carboxyl groups.

Grazing-incidence x-ray diffraction (GI-XRD)

GI-XRD measurements were carried out on a Bruker D8 Discovery diffractometer with Cu Kα source (X-ray wavelength, λ = 1.54 Å). To maximize signal from the films, 3 wt % PAA solutions were used for preparing the spin-coated films on a Si substrate with 100 nm oxide layer. Incidence angle was set at 0.5° and data was collected from 5° to 30° at 0.1° intervals with a dwell time of 4 seconds per data point. Fig. S5 shows the GI-XRD spectra for spin-cast PAA films at different pH.

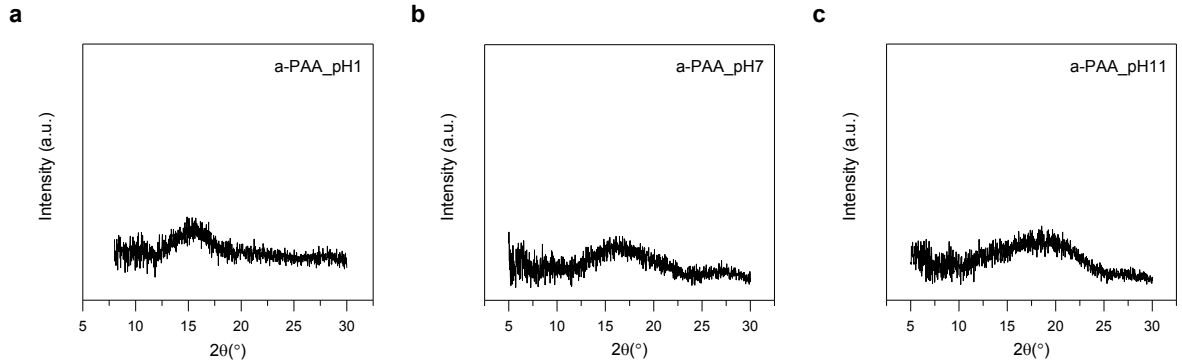

Fig. S5. GI-XRD spectra of PAA films at different pH | The broad diffused peak from ~15°–30°, called amorphous halo, is characteristic of amorphous polymers.

Calculation of Thermal Conductivity using MTCM Model

As mentioned in *Xie et.al* [3], the minimum thermal conductivity based on MTCM is:

$$\Lambda_{min} = \left(\frac{\pi}{6}\right)^{1/3} k_B \rho^{2/3} \sum_{i=1}^{3} V_i \left(\frac{T}{\Theta_i}\right) \int_0^{\Theta_i/T} \frac{x^3 e^x}{(e^x - 1)^2} dx \qquad (1)$$

Where k_B is the Boltzmann constant; ρ is the atomic density. In the high-temperature limit, the above equation can be simplified as [4]:

$$\Lambda_{min} = \left(\frac{\pi}{48}\right)^{\frac{1}{3}} k_B \rho^{\frac{2}{3}} (V_l + 2V_t) \qquad (2)$$

Where V_l and V_t are the longitudinal and transverse velocity of sound, respectively. The velocity of sound can on Elastic modulus *(E)* as follows [5]

$$\frac{1}{3}(V_l + 2V_t) \approx 0.94 \sqrt{E/\rho} \qquad (3)$$

Using this equation, it can be seen that Λ_{min} is dependent on the atomic density and Elastic modulus as

$$\Lambda_{min} = K_0 \rho^{\frac{1}{6}} \sqrt{E} \quad (4)$$

Where $K_0 = 2.82 k_B \left(\frac{\pi}{48}\right)^{\frac{1}{3}}$, is constant.

Here, in this study, we have experimentally measured the Elastic modulus of the polymer samples, as shown in Figure. 4. We have tried to measure the film density using X-ray reflectometry and gas pycnometer, but the data was not reliable for the analysis due to the thin thickness of our samples. Thus, to deconvolute the contribution of atomic density to the thermal conductivity enhancement for PAA polymer samples, we interpolated densities at different degrees of ionization based on the bulk densities reported in *Hiraoka et.al* [5]. By assuming that the film density scales linearly with the bulk density, a 14% higher bulk density at pH 11 (~90%) degree of ionization compared to pH 1 (20%) degree of ionization, suggested a relatively small (~2%) density related contribution to the enhanced thermal conductivity. However, the modulus related contribution to the measured thermal conductivity (κ) was calculated to be ~56%. On this basis of only the density and modulus related contributions to κ for a-PAA, the thermal conductivity at pH 11 is predicted to be ~0.72 W/m.K (as mentioned before), a 53% enhancement in κ over that of pH 1 sample (κ = 0.47 W/m.K), which was calculated using Eq (4) as follows:

At pH=1, $\kappa_1 = K_0 \rho_1^{1/6} \sqrt{E_1}$

At pH=11, $\kappa_{11} = K_0 \rho_{11}^{1/6} \sqrt{E_{11}}$

Using Figure.4, E_1 = *~22 GPa* and E_{11} = *~50 GPa*, and ρ_1 and ρ_{11} were interpolated from *Hiraoka et.al* [R4] which was observed to be *~1.5g/cm³* and *~1.7 g/cm³*, respectively. As the density related contribution to κ enhancement was observed to be negligible, it was ignored for PMAA.

References

[1] L. M. Fuhrer, S. Sun, V. Bokyo, M. Kellermeier, and H. Colfen, *Phys. Chem. Chem. Phys.*, 2020, **22**, 18631.

[2] D. G. Cahill, M. Katiyar, and J. R. Abelson, *Phys. Rev. B Cond. Matt.*, 1994, **50**, 6077-6081.

[3] X. Xie, K. Yang, D. Li, T. H. Tsai, J. Shin, P. V. Braun, and D. G. Cahill, *Phys. Rev. B*, 2017, **95**, 035406.

[4] W. P. Hsieh, M. D. Losego, P. V. Braun, S. Shenogin, P. Keblinski, and D. G. Cahill, *Phys. Rev. B*, 2011, **83**, 174205.

[5] M. T. Agne, R. Hanus, and G. J. Snyder, *Energy & Environmental Science*, 2018, **11**, 609.

[6] K. Hiraoka, H. Shin, and T. Yokoyama, *Polymer Bulletin*, 1982, **8**, 303-309.